arXiv:cond-mat/0611259v1 [cond-mat.other] 9 Nov 2006

Acoustic attenuation rate in the Fermi-Bose model with a finite-range fermion-fermion interaction

Bogdan Mihaila*
Theoretical Division, Los Alamos National Laboratory, Los Alamos, NM 87545 and
Materials Science and Technology Division, Los Alamos National Laboratory, Los Alamos, NM 87545

Sergio Gaudio
Department of Physics, Boston College, Chestnut Hill, MA 02167 and
Theoretical Division, Los Alamos National Laboratory, Los Alamos, NM 87545

Kevin S. Bedell
Department of Physics, Boston College, Chestnut Hill, MA 02167

Krastan B. Blagoev and Eddy Timmermans
Theoretical Division, Los Alamos National Laboratory, Los Alamos, NM 87545

We study the acoustic attenuation rate in the Fermi-Bose model describing a mixtures of bosonic and fermionic atom gases. We demonstrate the dramatic change of the acoustic attenuation rate as the fermionic component is evolved through the BEC-BCS crossover, in the context of a mean-field model applied to a finite-range fermion-fermion interaction at zero temperature, such as discussed previously by M.M. Parish *et al.* [Phys. Rev. B **71**, 064513 (2005)] and B. Mihaila *et al.* [Phys. Rev. Lett. **95**, 090402 (2005)]. The shape of the acoustic attenuation rate as a function of the boson energy represents a signature for superfluidity in the fermionic component.

PACS numbers: 03.75.Ss,05.30.Fk,32.80.Pj,67.90.+z

I. INTRODUCTION

Recent realization of superfluidity in a dilute gas of ultracold fermionic atoms, is driving renewed theoretical efforts aiming at a quantitative understanding of many-body correlations in a dilute Fermi gas. At low density, for finite-range interactions, one expects that all sensitivity to the detailed features of the interaction is lost [1], and the system's quantum behavior depends only on the scattering length and the range of the interaction. Furthermore, as we approach the "unitarity" limit [2], i.e. the limit where the scattering length is much larger than the mean inter-particle separation, the system exhibits universal behavior and the energy is determined entirely by the density, leading to high sensitivity to many-body correlation effects.

Built on the successful realization of quantum degenerate systems consisting of boson [3] and/or fermion [4] atoms, experimental progress in cold atom physics has recently resulted in the generation of ultracold molecules from ultracold atoms [5], Bose-Einstein condensates (BEC) of molecules [6], and the first experimental realization of the small pair to large pair crossover [7, 8, 9]. In one type of experiments [7, 8, 9], the system consists of one-type of cold, degenerate, fermionic atoms in an optical trap. The strength of the interatomic interaction can be continuously adjusted via a magnetically-tuned Feshbach resonance between a closed and an open channel. Hence, the system can evolve from a BEC phase in which spatially non-overlapping (Shafroth) pairs [10] are bound together, to a Bardeen-Cooper-Schrieffer (BCS)-type superfluid [11] involving correlated atom pairs in momentum space.

Significant experimental work has been also directed towards the study of mixtures of bosonic and fermionic atom gases [12, 13]. Such mixtures remind of the strongly correlated ^{3}He-^{4}He mixtures [14], and can be obtained by sympathetically cooling a gas of fermionic atoms by using a condensed boson gas as a refrigerator. In this paper, we will focuss on the latter type of system, and discuss the fermionic response to a density fluctuation of the Bose condensate in the trap, with special emphasis on the effects due to the finite-range character of the fermion-fermion interaction. We will argue that the shape of the acoustic attenuation rate depends on the BEC or BCS character of the fermionic liquid.

II. ACOUSTIC ATTENUATION IN THE FERMI-BOSE MODEL

The Hamiltonian describing the interacting Fermi-Bose system is given as the sum of a boson, fermion and interaction components

$$\mathbf{H}_{\rm FB} \ = \ \mathbf{H}_{\rm B} \ + \ \mathbf{H}_{\rm F} \ + \ \mathbf{H}_{\rm int} \, . \tag{1}$$

This model, proposed in this context by Timmermans *et al* [15], is similar to the a model introduced by Bardeen

---

*Electronic address: bmihaila@lanl.gov

et al [16] to describe the effect of the fluctuations of the polarization in an excitonic liquid and a gas of electrons. This model has since been the subject of intense investigations in connection with the Feshbach resonance mechanism in ultracold fermionic gases [17, 18].

In the weak coupling limit, the Fermi and Bose components can be treated independently, and the many-body wave function of the Fermi-Bose mixture is the direct product of *independent* Fermi and Bose wave functions, $|\Phi_{FB}\rangle = |\Phi_B, \Phi_F\rangle$. The dispersion relation of the dilute Bose condensate is [19]

$$\omega_q \;=\; c\, q\, \sqrt{1 + (\xi_B\, q)^2}\,, \tag{2}$$

where $c = \sqrt{\lambda_B\, \rho_B / m_B}$ is the phonon (BEC excitation) velocity of sound, $\xi_B = 1/\sqrt{4\lambda_B \rho_B m_B}$ is the boson coherence length, and $\lambda_B = 4\pi a_B / m_B$ is the strength of the bosonic pseudo-potential. The coherence length, i.e. the length scale at which the condensate varies spatially, is typically of the order of $\xi_B \sim 0.1 - 1\,\mu$m, while c is approximately $0.01\ \mu$m MHz in condensates with density of $100\,\mu\mathrm{m}^{-3}$. The scattering length, a_B, and the density of the bosonic component, ρ_B, are tunable parameters which can be used to modify the dispersion relation (2), but $c\,\xi_B = 1/(2\, m_B)$, $c/\xi_B = 2\, \lambda_B\, \rho_B \sim \rho_B\, a_B$ and, therefore, the parameters c and ξ_B cannot be varied independently. Throughout this paper $\hbar = 1$, i.e. the energy is measured in units of frequency.

The low-energy state of the system is described by the free-energy associated with the BCS-reduced Hamiltonian

$$\begin{aligned} \mathbf{H}_{\rm F} \;=\; & \sum_{\mathbf{k}} \epsilon_{\mathbf{k}} \left(a^\dagger_{\mathbf{k}\uparrow} a_{\mathbf{k}\uparrow} + a^\dagger_{\mathbf{k}\downarrow} a_{\mathbf{k}\downarrow} \right) \\ & + \sum_{\mathbf{k,p,q}} V_{\mathbf{q}}\; a^\dagger_{\mathbf{k}\uparrow} a^\dagger_{\mathbf{p}\downarrow} a_{\mathbf{p-q}\downarrow} a_{\mathbf{k+q}\uparrow}\,, \end{aligned} \tag{3}$$

with $\epsilon_{\mathbf{k}} = \mathbf{k}^2/(2m_F)$. Then, in a zero-temperature mean-field approximation [20, 21, 22], the fermionic ground-state in the Hartree-Fock-Bogoliubov representation [23] is the standard BCS variational wave function given by

$$|\Phi_F\rangle \;=\; \mathcal{N}\ \exp\left(\sum_{\mathbf{k}} \frac{v_{\mathbf{k}}}{u_{\mathbf{k}}}\ a^\dagger_{\mathbf{k}\uparrow} a^\dagger_{-\mathbf{k}\downarrow} \right)\ |0\rangle\,. \tag{4}$$

The BCS ansatz interpolates smoothly between the BCS and BEC limit. The parameters $\{u_{\mathbf{k}},\, v_{\mathbf{k}}\}$ are obtained by solving the system of equations $v^2_{\mathbf{k}} = \frac{1}{2} - (\epsilon_{\mathbf{k}} - \mu)/(2E_{\mathbf{k}})$ and $u_{\mathbf{k}} v_{\mathbf{k}} = \Delta_{\mathbf{k}}/(2E_{\mathbf{k}})$, subject to the normalization condition, $|u_{\mathbf{k}}|^2 + |v_{\mathbf{k}}|^2 = 1$. Here, μ is the fermionic chemical potential such that spin-up and spin-down states are equally occupied, and $E_{\mathbf{k}}$ denotes the quasi-particle spectrum in the fermionic ground state, $E^2_{\mathbf{k}} = (\epsilon_{\mathbf{k}} - \mu)^2 + \Delta^2_{\mathbf{k}}$. The pairing gap, $\Delta_{\mathbf{k}}$, is obtained as $\Delta_{\mathbf{k}} = -\sum_{\mathbf{p}} V_{\mathbf{k-p}}\, \Delta_{\mathbf{p}}/E_{\mathbf{p}}$.

The interaction between the Fermi and Bose components is assumed to be weak, and the interaction Hamiltonian, $\mathbf{H}_{\rm int}$, describing the interaction of a single acoustic phonon of momentum $\mathbf{q}$ and energy ω_q with the fermionic component can be written similarly to the electron-phonon Hamiltonian [24], as:

$$\mathbf{H}_{\rm int} \sim \sqrt{\frac{1}{2\rho\, \omega_q}}\ \int \frac{\mathrm{d}^3 k}{(2\pi)^3}\ |\mathbf{q}|\ \mathbf{b}^\dagger_{\mathbf{q}} \sum_{\sigma=\uparrow,\downarrow} \mathbf{a}^\dagger_{\mathbf{k-q},\sigma}\, \mathbf{a}_{\mathbf{k}\sigma}\ +\ \text{h.c.}\,, \tag{5}$$

where ρ is the mass density of the composite gas. (For an alternate approach based on a density-density interaction, see Ref. [25].) In first-order perturbation theory [26], the acoustic attenuation rate is given by

$$\Gamma(q) \;=\; 2\pi\ |\, \langle i | \mathbf{H}_{\rm int} | f \rangle \,|^2\ \delta(E_i - E_f)\,. \tag{6}$$

At zero temperature, for a spin-unpolarized Fermi gas, we obtain [24]:

$$\begin{aligned} \Gamma(q) & \sim \frac{q^2}{\omega_q}\ \left[\gamma_\rho(q) + \gamma_\kappa(q) \right] \qquad\qquad (7) \\ & \sim \frac{q^2}{\omega_q} \int \frac{\mathrm{d}^3 k}{(2\pi)^3} \left[\rho_{\mathbf{k}} (1 - \rho_{\mathbf{k}'}) + \kappa_{\mathbf{k}} \kappa_{\mathbf{k}'} \right] \delta(\omega_q - E_k - E_{k'})\,, \end{aligned}$$

with $\mathbf{k}' = \mathbf{q} + \mathbf{k}$. In the mean-field approximation, the normal and anomalous densities in the fermionic ground state are defined as $\rho_{\mathbf{k}} = \langle \Phi | \mathbf{a}^\dagger_{\mathbf{k}\uparrow} \mathbf{a}_{\mathbf{k}\uparrow} | \Phi \rangle = |v_{\mathbf{k}}|^2$, and $\kappa_{\mathbf{k}} = \langle \Phi | \mathbf{a}_{-\mathbf{k}\downarrow} \mathbf{a}_{\mathbf{k}\uparrow} | \Phi \rangle = v^*_{\mathbf{k}} u_{\mathbf{k}}$. The acoustic attenuation rate appears as the superposition of components γ_ρ and γ_κ, which depend separately on the normal and anomalous densities, respectively (see also Ref. [27]).

In principle, one should also consider the possibility of exciting the Anderson-Goldstone mode of the fermion superfluid system. However, as it has been discussed in Ref. [25], the Anderson-mode excitation can be avoided by specifying that the BEC velocity of sound, c, is less than the velocity of the Anderson mode, v, i.e. we require $c < v$. Then, the excitation of the collective Anderson mode by a BEC phonon mode is energetically forbidden. This is a reasonable assumption for the mixtures of bosonic BEC and fermionic atom gases under consideration here: In the BCS regime, the velocity of the Anderson mode, v, is equal to the Fermi-velocity v_F and, for typical atom trap conditions, that can be easily satisfied. The only cold atom mixtures for which $c > v_F$ contain ultra-low density fermion systems or ultra-high density BEC's: the first type would be difficult to realize because of the very low critical temperature for fermion superfluidity, the second type would be difficult to achieve experimentally because three-body recombination processes would quickly deplete the experimental system. Hence, while the Anderson mode will most likely be somewhat softened in the crossover regime (since we expect it to go over into the Bogoliubov mode of the BEC-system in the BEC limit of the crossover), by choosing a sufficiently weakly interacting BEC or low density BEC, it should always be possible to ensure that $c < v$ throughout the entire crossover.

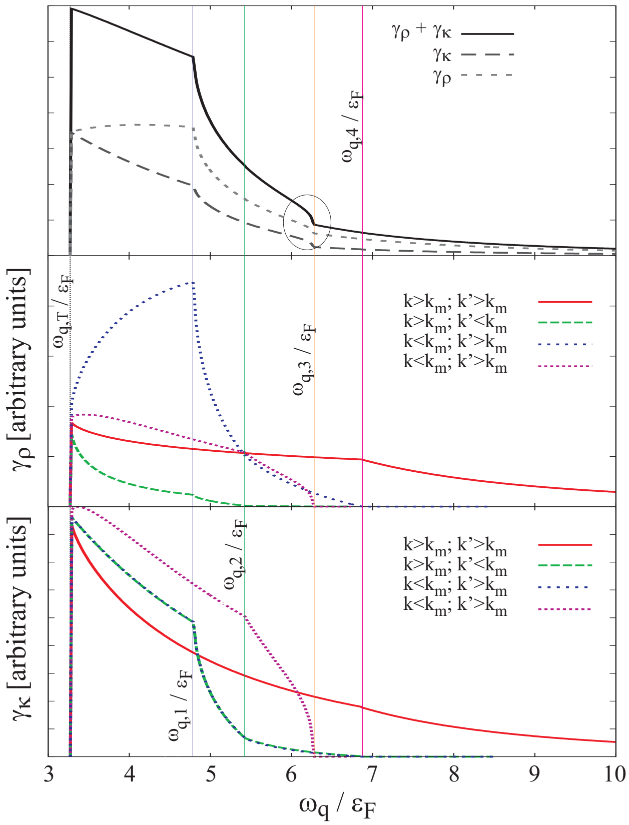

FIG. 1: (Color online) Acoustic attenuation rate components corresponding to the toy model described by Eq. (8). Here we study a large pairing-gap, Δ_0/ε_F, regime: we set $\Delta_0/\varepsilon_F = 4$, $\mu/\varepsilon_F = 1$, and $\xi_B k_F = 5$.

III. A SIMPLE MODEL

In order to study the phase-space constraints subjecting the acoustic attenuation rate, we consider first a schematic model of the momentum-dependence of the pairing gap, suggested by Comte and Nozières [21]:

$$\Delta_k \;=\; \frac{\Delta_0}{1+(k/k_F)^2}\,. \tag{8}$$

Note that the realistic momentum dependence of the pairing gap, as predicted by the one-channel fermion-fermion model with a finite-range interaction to be discussed in the next section, has a much longer tail than the simple ansatz of Comte and Nozières [21]. Unless otherwise specified, in the following we set $\hbar c k_F/\varepsilon_F = 1$ for simplicity. We also keep fixed the chemical potential, μ/ε_F, and the coherence length of the Bose-gas component, $\xi_B k_F$, and vary the pairing-gap parameter Δ_0/ε_F.

For illustrative purposes, in Figs. 1 and 2, we plot the energy-dependence of the various attenuation-rate components, γ_κ and γ_ρ, for the regime of large and small values of the pairing-gap, Δ_0/ε_F, respectively. Because the quasi-particle spectrum in the model described by Eq. (8) has a minimum at finite momentum, k_m, then the conservation of energy, $E_{k'} = \omega_q - E_k$, and momentum, $\mathbf{k}' = \mathbf{q} + \mathbf{k}$, leads to four branches. The available phase-space satisfying these constraints leads to kinks observed in the energy-dependence of the acoustic attenuation rate. In particular, we have four "critical" points, as depicted by the vertical lines in Figs. 1 and 2. In the increasing order of the "critical" energy, we have:

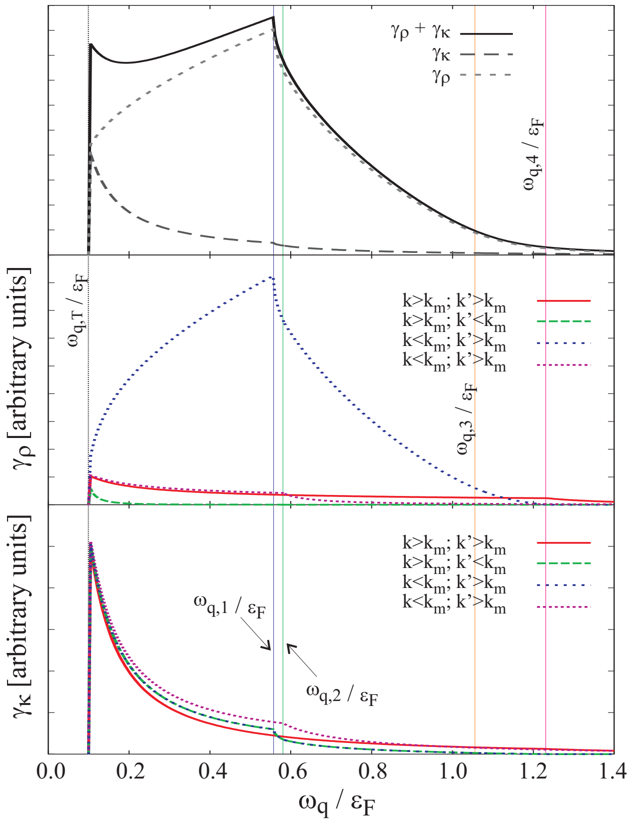

FIG. 2: (Color online) Acoustic attenuation rate components corresponding to the toy model described by Eq. (8). Here we study a small pairing-gap, Δ_0/ε_F, regime (BCS-like): we set $\Delta_0/\varepsilon_F = 0.1$, $\mu/\varepsilon_F = 1$, and $\xi_B k_F = 5$.

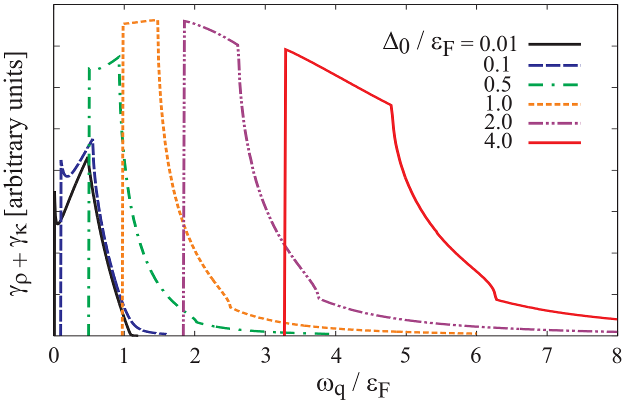

FIG. 3: (Color online) Shapes of the energy-dependence of the attenuation-rate as a function of the pairing-gap parameter, Δ_0/ε_F, for fixed values of $\mu/\varepsilon_F = 1$ and $\xi_B k_F = 5$.

$\omega_{q,1}$ the energy value at which the momentum conservation corresponding to the second ($k > k_m,\ k' < k_m$) and third ($k < k_m,\ k' > k_m$) branches, is no longer satisfied. This failure generates the most remarkable feature in the acoustic attenuation rate, resulting in a decrease in the acoustic attenuation rate; $\omega_{q,2}$ the energy value at which the fourth branch ($k < k_m,\ k' < k_m$) also fails due to failed momentum conservation; $\omega_{q,3}$ the energy value at which the fourth branch vanishes; and $\omega_{q,4}$ the energy value at which the second and third branches also vanish: from this point on, the only contribution is from the first branch ($k > k_m,\ k' > k_m$).

The energy distribution of the acoustic attenuation rate may feature a "shoulder" just before $\omega_{q,3}$, because the domain of the integrals corresponding to branches three and four is $k \in [0, k_m]$, i.e. the integration domain for these branches is ω_q-independent (see circled area in the top panel of Fig. 1. This "shoulder" is apparent in the large Δ_0/ε_F regime, and disappears as we approach the normal Fermi gas limit.

In the small Δ_0/ε_F regime, the "critical" energies $\omega_{q,1}$ and $\omega_{q,2}$ are close together, while the "critical" energies $\omega_{q,3}$ and $\omega_{q,4}$ are pushed to relatively higher values. When Δ_0/ε_F becomes very small, only one of the eight contributions to Γ is significant (due to the fact that the anomalous density is a delta-like distribution centered around k_F), and the kinks in the energy distribution of the acoustic attenuation rate are entirely obscured, except for $\omega_{q,1}$.

In Fig. 3 we show evolution of the attenuation rate profile as a function of the pairing-gap, Δ_0/ε_F, at fixed chemical potential. The shape of the attenuation rate changes smoothly between low and large values of the pairing-gap. The signature of the crossover is the change in the sign of the slope of the acoustic attenuation rate, for phonon energies between the threshold energy, $\omega_{q,T} = 2E_{k_\mathrm{m}}$, and the first "critical" value, $\omega_{q,1}$: the slope is positive in the small Δ_0/ε_F regime, and becomes negative in the large Δ_0/ε_F regime. From Figs. 1 and 2 follows that , the crossover is characterized by the ratio of $\gamma_\kappa/\gamma_\rho$, i.e. the ratio of the anomalous- to the normal-density. In the small Δ_0/ε_F limit this ratio is small (it vanishes for the Fermi gas). In the large Δ_0/ε_F limit, the anomalous-density contribution is comparable in size (but still smaller) than the normal-density contribution. In the limit when $\Delta_0 \to 0$, we recover the normal Fermi gas result.

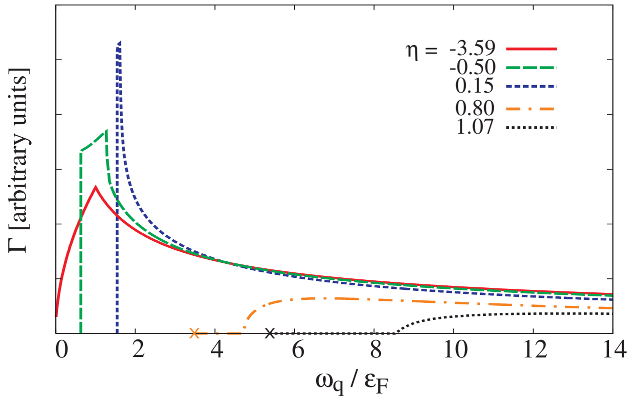

FIG. 4: (Color online) Energy dependence of the acoustic attenuation rate as the fermionic component goes through the BEC-BCS crossover, for the choice of parameters in Ref. [22]. Along the ω_q-axis, we plot the position of the energy thresholds, $\omega_{q,T} = 2E_{k_\mathrm{m}}$.

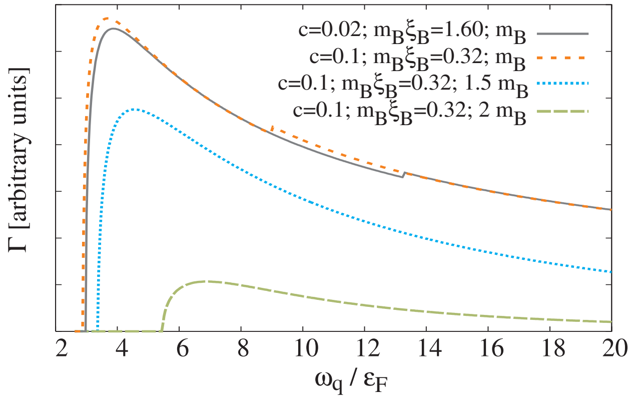

FIG. 5: (Color online) Effect of the bosonic parameters on intensity of the BEC signal.

IV. EFFECTS OF A FINITE-RANGE FERMION-FERMION INTERACTION

We consider now a more realistic scenario, in which the fermionic atoms interacting via a short-range Gaussian potential, $V(r) = V_0 \exp(-br^2)$. The mean-field approximation for the ground-state properties of this system has been discussed recently in Ref. [22], where the BEC-BCS crossover was studied by fixing the width of the potential $\langle r\rangle = 2/\sqrt{\pi b}$ and varying the potential depth V_0, or implicitly the scattering length a_F of the interaction. Following Leggett [20], the dilute fermionic state is characterized by the parameter $\eta = (k_F a_F)^{-1}$, which combines together the density of the fermionic gas, characterized by the Fermi momentum, k_F, and the fermion-fermion scattering length. The BEC-BCS crossover is indicated by the disappearance of the singularity in the fermionic density of states, $N(k) \sim k^2 \left|\frac{\mathrm{d}E_k}{\mathrm{d}k}\right|^{-1}$ (see Fig. 3 in Ref. [22]). These results are similar to a magnetic field dependent contact interaction [28], and are relevant to present experiments in which only the lowest hyperfine levels of the fermionic atom gas are populated.

To study the effect of the energy-momentum dependence of the normal and anomalous densities on the acoustic attenuation rate, we consider the BEC-BCS crossover at constant-density corresponding to $k_F\langle r\rangle \approx 0.37$. The BEC-BCS crossover in this case occurs for $\eta = (k_F a_F)^{-1}$ between 0.15 and 0.80. We assume that the dispersion relation of the bosonic component is given by the parameters: $c = 0.02\,\mu\mathrm{m\,MHz}$, and $m_B\xi_B = 1.6\,(\mathrm{u})(\mu\mathrm{m})$. Our results are illustrated in Fig. 4. Here, the energy dependence of the attenuation rate, Γ, as a function of the scattering length (or $\eta = (k_F a_F)^{-1}$), is plotted at fixed fermion density ($k_F\langle r\rangle \approx 0.37$). For our choice of parameters in the dispersion relation of the dilute Bose condensate (see Eq. (2)), the ratio q^2/ω_q approaches a constant for $\omega_q/\varepsilon_F \ll 1$. Here k_F is the Fermi momentum, and a_F is the s-wave scattering length in the fermionic component.

At the threshold, on the BCS side, the acoustic attenuation rate features a sharp edge, followed by a (linear) increase in the acoustic attenuation rate as a function of the phonon energy; in contrast, on the BEC side, the sharp edge is smoothed out, and the acoustic attenuation rate decreases slowly as a function of energy. It is important to recall that in the dilute limit the BEC-BCS crossover coincides with the singularity in the scattering length, and occurs for $\mu = 0$ [20]. The acoustic attenuation rate provides a crisp signature of the BEC-BCS crossover.

On the BEC side, the energy threshold in first-order perturbation theory is higher than the energy threshold ($\omega_{q,T} = 2E_{k_\mathrm{m}}$) given by energy conservation, due to the reduced phase space availability for momentum conservation. In this regime we have $k_m = 0$ and the contributions due to the third and fourth branches ($k < k_m$) vanish. Due to the lack of available phase space for the integral (7), the actual threshold in first-order perturbation theory is located further away from the energy threshold as we go deeper into the BEC regime (see Fig. 4). The effect is enhanced by a smaller bosonic coherence length.

From the numerical results depicted in Fig. 4 it is apparent that the attenuation rate calculated in first-order perturbation theory vanishes in the deep BEC region. In this regime, one needs to include a second-order approximation in order to describe the scattering of the boson off the molecular condensate. Provided that i) the molecular condensate degrees of freedom do not play a role and that ii) the coupling between the bosonic and fermionic components is sufficiently weak this second-order correction in perturbation theory is expected to be small and will not be discussed here. For energies greater than the threshold, the acoustic attenuation rate becomes nonzero and the first-order result is expected to be dominant.

The dependence on the phonon velocity and/or the boson mass of the strength of the BEC signal is illustrated in Fig. 5. Here, we depict the acoustic attenuation rate for $\eta = 0.59$ (the crossover region), as obtained by first changing the phonon velocity from 0.02 to 0.1 μm MHz, which is equivalent to changing $m_B\xi_B$ from 1.6 to 0.32 (u)(μm). Next, we increase the boson mass, m_B, first by 50 % and then by 100 %, which is equivalent to reducing by the same factor the bosonic coherence length, ξ_B. The acoustic attenuation rate changes little when we increase the phonon velocity, c, for a given boson mass, m_B. In contrast, for heavier bosons, the signal drops in intensity very quickly for a relatively small increase of the boson mass, or else for a relatively small decrease in the bosonic coherence length.

We note that in a related formalism, similar shapes (especially on the BEC side) are present in the discussion of the spin-spin correlation functions (see Refs. [27, 29]). These calculations refer to observables accessible via Bragg, rf and spin-noise spectroscopy. Therefore, measurements of the acoustic attenuation rate can be used in conjunction with these other techniques to probe features of the fermionic normal and anomalous densities. The acoustic attenuation rate discussed here is intrinsically a nonzero momentum transfer measurement, thus probing different moments of the fermionic normal and anomalous densities. This in turn results in different features in the shapes on the BCS side.

V. CONCLUSIONS

To summarize, in this paper we have studied the acoustic attenuation rate in the framework of the Fermi-Bose model, for a realistic finite-range fermion-fermion interaction. Our findings suggest that by inducing a density fluctuation in the Bose gas component one can induce an acoustic response in the fermionic component, and the shape of the acoustic attenuation rate can be used as a signature of superfluidity on the BCS side. For a low excitation energy, the acoustic attenuation rate increases with the phonon energy on the BCS side and decreases on the BEC side. Therefore, a linear increase of the acoustic attenuation rate with the phonon energy above the threshold indicates that one has passed to the BCS side. Moreover, our results show that the signal on the BCS side is much larger than on the BEC side, which makes the detection easier. The acoustic attenuation rate measurement is favored by a larger phonon velocity and the choice of the lightest available boson specie.

Acknowledgments

This work was supported in part by the LDRD program at Los Alamos National Laboratory. B.M. acknowledges financial support from an ICAM fellowship program. The authors would like to thank M.M. Parish, P.B. Littlewood, and D.L. Smith for useful discussions.

---

[1] L.I. Schiff, *Quantum Mechanics* (McGraw-Hill, New York, 1968).
[2] G.A. Baker, Phys. Rev. C **60**, 054311 (1999); T. Papenbrock and G.F. Bertsch, *ibid.* **59**, 2052 (1999); H. Heiselberg, Phys. Rev. A **63**, 043606 (2001); R. Combescot, Phys. Rev. Lett. **91**, 120401 (2003); J. Carlson, S.-Y.

Chang, V.R. Pandharipande, and K.E. Schmidt, *ibid.* **91**, 050401 (2003).

[3] M.H. Anderson *et al.*, Science **269**, 198 (1995); K.B. Davis *et al.*, Phys. Rev. Lett. **75**, 3969 (1995); C.C. Bradley, C.A. Sackett, J.J. Tollett, and R.G. Hulet, *ibid* **75**, 1687 (1995).

[4] B. DeMarco and D.S. Jin, Science **285**, 1703 (1999).

[5] C.A. Regal, C. Ticknor, J.L. Bohn, and D.S. Jin, Nature (London) 424, 47 (2003).

[6] C.A. Regal, C. Ticknor, J.L. Bohn, and D.S. Jin, Nature (London) **424**, 47 (2003); M.W. Zwierlein *et al.*, Phys. Rev. Lett. **91**, 250401 (2003). Bartenstein *et al.*, *ibid.* **92**, 120401 (2004); T. Bourdel *et al.*, *ibid.* **93**, 050401 (2004), G.B. Partridge, K.E. Strecker, R.I. Kamar, M.W. Jack, and R.G. Hulet, *ibid.* **95**, 020404 (2005).

[7] C. A. Regal, M. Greiner, and D. S. Jin, Phys. Rev. Lett. **92**, 040403 (2004).

[8] M. Bartenstein *et al.*, Phys. Rev. Lett. **92**, 203201 (2004); M. W. Zwierlein *et al.*, Nature (London) **435**, 1047 (2005).

[9] M. W. Zwierlein *et al.*, Phys. Rev. Lett. **92**, 120403 (2004).

[10] M. R. Shafroth, S. T. Butler, and J. M. Blatt, Helv. Phys. Acta, **30**, 93 (1957); M. R. Shafroth, Phys. Rev. **111**, 72 (1958); P. Nozières and S. Schmitt-Rink, J. Low Temp. Phys. **59**, 195 (1985).

[11] J. Bardeen, L. N. Cooper, and J. R. Schrieffer, Phys. Rev. **106**, 162 (1957); *ibid.* Phys. Rev. **108**, 1175 (1957).

[12] C.A. Stan, M.W. Zwierlein, C.H. Schunck, S.M.F. Raupach, and W. Ketterle, Phys. Rev. Lett. **93**, 143001 (2004).

[13] S. Inouye *et al.*, Phys. Rev. Lett. **93**, 183201 (2004).

[14] E. Krotscheck and M. Saarela, Phys. Rep. **232**, 1 (1993).

[15] E. Timmermans, Contemp. Phys. **42**, 1 (2001); E. Timmermans, K. Furuya, P. W. Milonni, and A. K. Kerman, Phys. Lett. A **285**, 228 (2001); E. Timmermans, P. Tommasini, M. Hussein, and A. K. Kerman, Phys. Rep. **315**, 199 (1999).

[16] D. Allender and J. Bardeen, Phys. Rev. B **7**, 1020 (1973); J. C. Inkson and P. W. Anderson, *ibid.* **8**, 4429 (1973); D. Allender, J. Bray, and J. Bardeen, *ibid.* **8**, 4433 (1973).

[17] Y. Ohashi and A. Griffin, Phys. Rev. Lett. **89**, 130402 (2002); Phys. Rev. A **67**, 033603 (2003); *ibid.* **67**, 063612 (2003).

[18] M. Holland, S.J.J.M.F. Kokkelmans, M. L. Chiofalo, and R. Walser, Phys. Rev. Lett. **87**, 120406 (2001); M. L. Chiofalo, S.J.J.M.F. Kokkelmans, J. N. Milstein, and M. J. Holland, *ibid.* **88**, 090402 (2001); S.J.J.M.F. Kokkelmans, J. N. Milstein, M. L. Chiofalo, R. Walser, and M. J. Holland, Phys. Rev. A **65**, 053617 (2002); J. N. Milstein, S.J.J.M.F. Kokkelmans, and M. J. Holland, *ibid.* **66**, 043604 (2002).

[19] E. Timmermans, Contemp. Phys. **42**, 1 (2001).

[20] A. J. Leggett, in *Modern Trends in the Theory of Condensed Matter*, edited by A. Pekalski and R. Przystawa (Springer-Verlag, Berlin, 1980).

[21] C. Comte and P. Nozières, J. Phys. (Paris) **43**, 1069 (1982).

[22] M. M. Parish, B. Mihaila, E. M. Timmermans, K. B. Blagoev, and P. B. Littlewood, Phys. Rev. B **71**, 064513 (2005).

[23] N. N. Bogoliubov, Nuovo Cimento **7**, 794 (1958); J. G. Valatin, Nuovo Cimento **7**, 843 (1958);

[24] G. D. Mahan, *Many-Particle Physics* (Plenum Press, New York, 1981).

[25] S. Gaudio, B. Mihaila, K. B. Blagoev, K. S. Bedell, and E. Timmermans, cond-mat/0512134.

[26] Perturbation theory with quasi-particle states is perfectly valid even if the system is strongly interacting: quasi-particle states interact weakly with each other, even if the underlying (real) fermions of the system interact strongly. Here, the expectation approach is that the quasi-particle picture remains valid for low-energy fermion modes even if the fermions become strongly interacting. This is the case for normal fermion systems, and this phenomenon, in which the Pauli-principle plays a major role, forms the basis of the Landau description of Fermi-liquid theory. In this case, a single low-energy fermion quasi-particle state near the gap could remain long lived as well, for reasons of kinematics and fermion statistics.

[27] B. Mihaila, S. Gaudio, K.B. Blagoev, A.V. Balatsky, P.B. Littlewood and D.L. Smith, Phys. Rev. Lett. **95**, 090402 (2005); B. Mihaila, S.A. Crooker, K.B. Blagoev, D.G. Rickel, P.B. Littlewood, D.L. Smith Phys. Rev. A (in press), e-print cond-mat/0601011.

[28] M. H. Szymanska, K. Goral, T. Kohler, and K. Burnett, Phys. Rev. A **72**, 013610 (2005).

[29] Similar line shapes were noted by H.P. Büchler, P. Zoller, and W. Zwerger, Phys. Rev. Lett. **93**, 080401 (2004), and R.B. Diener and T.-H. Ho, *e-print* cond-mat/0405174.